NASA TECHNICAL MEMORANDUM

NASA TM X-1518

NASA TM X-1518

DESCRIPTION AND FLIGHT PERFORMANCE RESULTS OF THE WASP SOUNDING ROCKET

by Joseph A. Yuska, James F. DePauw, and Lowell E. Steffens

Lewis Research Center

Cleveland, Ohio

NATIONAL AERONAUTICS AND SPACE ADMINISTRATION • WASHINGTON, D. C. • FEBRUARY 1968

NASA TM X-1518

DESCRIPTION AND FLIGHT PERFORMANCE RESULTS OF THE WASP SOUNDING ROCKET

By Joseph A. Yuska, James F. DePauw, and Lowell E. Steffens

Lewis Research Center
Cleveland, Ohio

NATIONAL AERONAUTICS AND SPACE ADMINISTRATION

For sale by the Clearinghouse for Federal Scientific and Technical Information
Springfield, Virginia 22151 – CFSTI price $3.00

DESCRIPTION AND FLIGHT PERFORMANCE RESULTS OF THE WASP SOUNDING ROCKET

by Joseph A. Yuska, James F. DePauw, and Lowell E. Steffens

Lewis Research Center

SUMMARY

A general description of the design and construction of the WASP sounding rocket and of the performance of its first flight are presented. The purpose of the flight test was to place the 862-pound (391-kg) spacecraft above 250 000 feet (76.25 km) on free-fall trajectory for at least 6 minutes in order to study the effect of "weightlessness" on a slosh dynamics experiment. The WASP sounding rocket fulfilled its intended mission requirements. The sounding rocket approximately followed a nominal trajectory. The payload was in free fall above 250 000 feet (76.25 km) for 6.5 minutes and reached an apogee altitude of 134 nautical miles (248 km).

Flight data including velocity, altitude, acceleration, roll rate, and angle of attack are discussed and compared to nominal performance calculations. The effect of residual burning of the second stage motor is analyzed. The flight vibration environment is presented and analyzed, including root mean square (RMS) and power spectral density analysis.

INTRODUCTION

To further "zero-gravity" research at the Lewis Research Center, an inexpensive sounding rocket was required capable of launching a 1000- to 1600-pound (454- to 725-kg) gross payload with a large payload envelope for at least 6 minutes coasting flight time above 250 000 feet (76.25 km) altitude into "free fall." The specific spacecraft was one to conduct a slosh dynamics study of a 22-inch-diameter (0.56-m-diam.) by 44-inch-long (1.12-m-long) baffled plexiglass tank partially filled with alcohol. Reference 1 describes the spacecraft and mission of the flight in detail. At the time the project was started a search for a flight-tested vehicle meeting all of the aforementioned requirements was unsuccessful, so development of the WASP vehicle was undertaken.

The WASP sounding rocket design was influenced by the fact that two first-stage assemblies were available from the Shotput program. Because the WASP project was a short program with only a few flights, it was expedient to design the vehicle around this existing hardware. The WASP sounding rocket then represented a useful collection of hardware capable of performing the mission.

The WASP is a two-stage, solid-propellant, unguided, spin-stabilized sounding rocket, 31.5 inches (0.8 m) in diameter and 580 inches (14.7 m) long including the 207-inch-long (5.25-m-long) payload compartment used in this flight. This classes it as larger than the Aerobees but smaller than Scout vehicles. Spin stabilization is achieved by the fixed cant of fins on both the first and second stages. In this flight, a requirement existed that the payload be nonspinning; therefore, a spin isolator was used to keep the payload from spinning while the vehicle rotated. From a vehicle standpoint, the payload could have been spun with no significant change in performance.

Propulsion for the WASP sounding rocket consisted of a 55 000-pound-thrust (244 600-N-thrust) "Pollux" XM33E6 plus two 35 000-pound-thrust (155 700-N-thrust) "Recruit" XM19E1 rocket motors for the first stage and a 23 000-pound-thrust (102 300-N-thrust) "Antares" X259A2 rocket motor for the second stage. Upon nearly simultaneous ignition at T-zero, the Recruits burned out at 2.4 seconds and the Pollux burned for 33 seconds. Staging was accomplished by explosively releasing a "V-clamp" at 35 seconds. The second stage ignited at 38.5 seconds and burned out at 76 seconds. Spacecraft housing and spacecraft separation occurred at 95 seconds, and spacecraft housing ejection took place at 97 seconds after lift-off.

The WASP sounding rocket was launched from NASA Wallops Station, Wallops Island, Virginia on June 7, 1966. With its 1528-pound (693-kg) payload, it achieved an altitude of 134 nautical miles (248 km) and a range of 295 nautical miles (546 km). This gave a zero-gravity test time of 6.5 minutes.

The present report will describe the flight configuration and construction details of the WASP sounding rocket in sufficient detail to interpret the flight results. The flight results reported are from the first WASP sounding rocket launched and in many cases are compared to nominal expected performance.

SYMBOLS

C_A axial-force coefficient at zero normal force

C_{N_η} normal-force coefficient slope at zero normal force, per radian

g acceleration due to gravity, 32.172 ft/sec^2 (9.8 m/sec^2)

M_o free-stream Mach number

q dynamic pressure, lb/ft^2 (N/m^2)

X_{cp} center of pressure at zero normal force (measured from station 0.0), in. (m)

α pitch angle of attack, deg

β yaw angle of attack, deg

η total angle of attack, $\sqrt{\alpha^2 + \beta^2}$, deg

VEHICLE DESCRIPTION

Construction Details

The WASP is a two-stage, solid-propellant, unguided, spin-stabilized sounding rocket 31.5 inches (0.8 m) in diameter and 580 inches (13.4 m) long including the 207-inch-long (5.25-m-long) payload compartment used in this flight. The outline of the WASP sounding rocket with the fluid dynamics experiment payload is shown in figure 1. A pic-

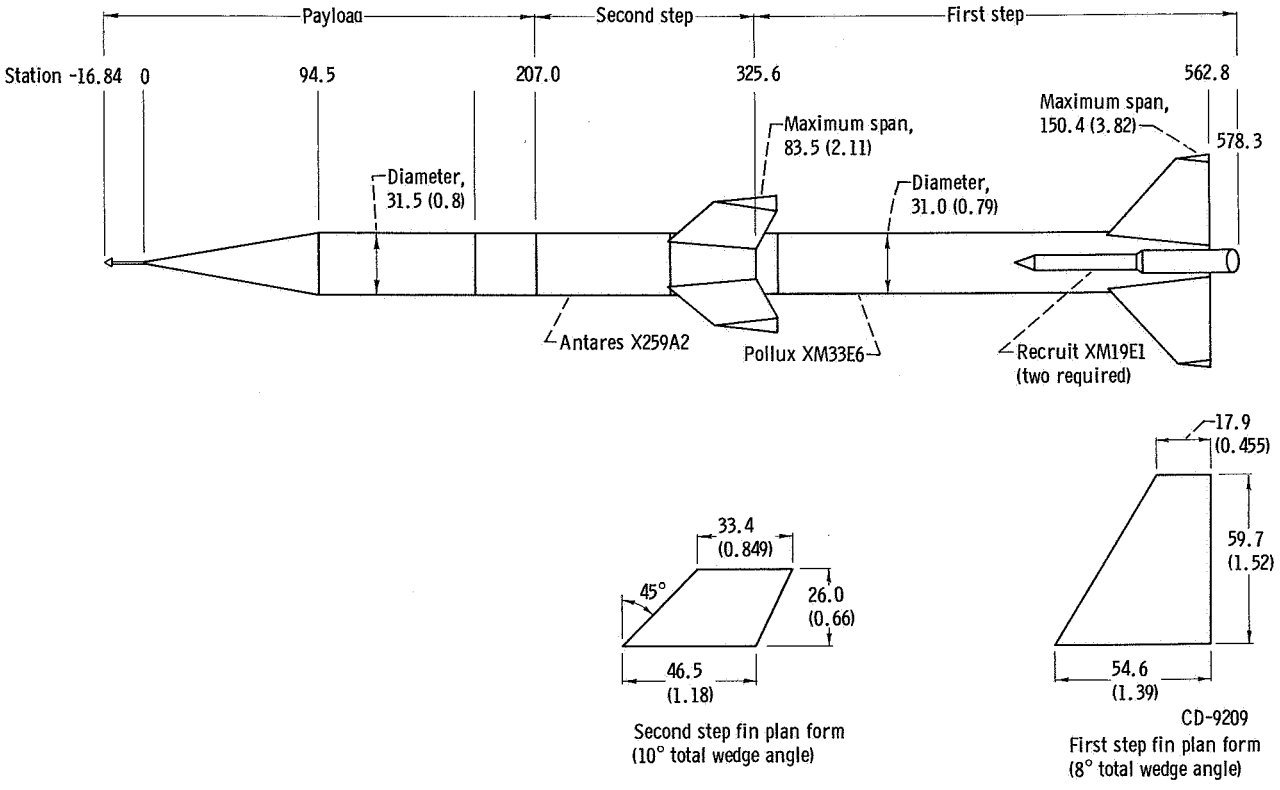

Figure 1. - Outline of WASP sounding rocket with fluid dynamics experiment payload. (All dimensions in inches (meters) unless noted otherwise.)

ture of this configuration on a zero-length guidance tubular launcher at Wallops Island is shown in figure 2.

First stage. - The first stage was identical to the Shotput first stage and consisted of a Pollux XM33E6 motor and two Recruit motors XM19E1 with nozzles canted outward at $6\frac{1}{2}^{\circ}$. The first-stage, 15-square-foot (1.39-m^2) wedge fins and supporting shroud were fabricated of cast and welded magnesium. The fins were canted at 2.0° to give the sounding rocket a clockwise spin when viewed from the launcher. Figure 3 is a picture of the assembled first stage.

Interstage structure. - The first- to second-stage interstage structure is shown in figure 4. It contained the first-stage thrust fitting, the stage-separation V-clamp, and the second-stage fin shroud which supported the $7\frac{1}{2}$-square-foot (0.695-m^2) wedge fins. The second-stage fins were canted at 50.5 minutes to induce spin in the same direction as the first-stage fins. The fins were of lightweight, riveted aluminum aircraft-type construction. Heat protection for the fins from aerodynamic heating was provided by an Inconel cap on the fin leading edge plus a 0.050-inch-thick (1.3-mm-thick) layer of ablative cork on the lifting surfaces. The fin trailing-edge surface had a 0.125-inch-thick (3.2-mm-thick) layer of ablative cork to resist heating from the exhaust plume.

Stage separation was accomplished by detonation of the four tangential explosive bolts that held the four-segment V-clamp together. The drag differential between the separated first- and second-stage payload combination provided the separation force. The V-clamp was machined from a forged aluminum ring. To prevent damage to the fins on release of the V-clamp segments, each V-clamp segment was secured to the first-stage thrust fitting by two short chains so that the V-clamp segments could release and move radially outward approximately only 1 inch (25.4 mm) upon bolt detonation.

Second stage. - The motor for the second stage was a filament-wound, fiberglass-cased Antares X259A2. The motor has a maximum temperature limitation of 100° F (311° K); therefore, heat protection for the motor was provided by a fiberglass insulation blanket taped around the casing, which was then covered by a 0.032-inch-thick (0.81-mm-thick) cylindrical aluminum fairing (see fig. 4). The fairing was secured to the payload-WASP sounding rocket interstage structure with radial screws at the forward edge while the aft edge was free to move longitudinally.

Figure 5 shows the assembled second stage without the fiberglass insulation blanket and fairing which were installed after the second stage was mated to the first stage on the launcher.

Payload support structure. - The second stage to payload interstage structure along with the spin isolator section of the gross payload is shown in figure 6. The batteries, timers, and electrical circuitry which accomplished stage separation and second-stage ignition were mounted in the payload adapter section, shown in figure 5(a). The four-segment V-clamp at station 215 was assembled with nonexplosive bolts because this sep-

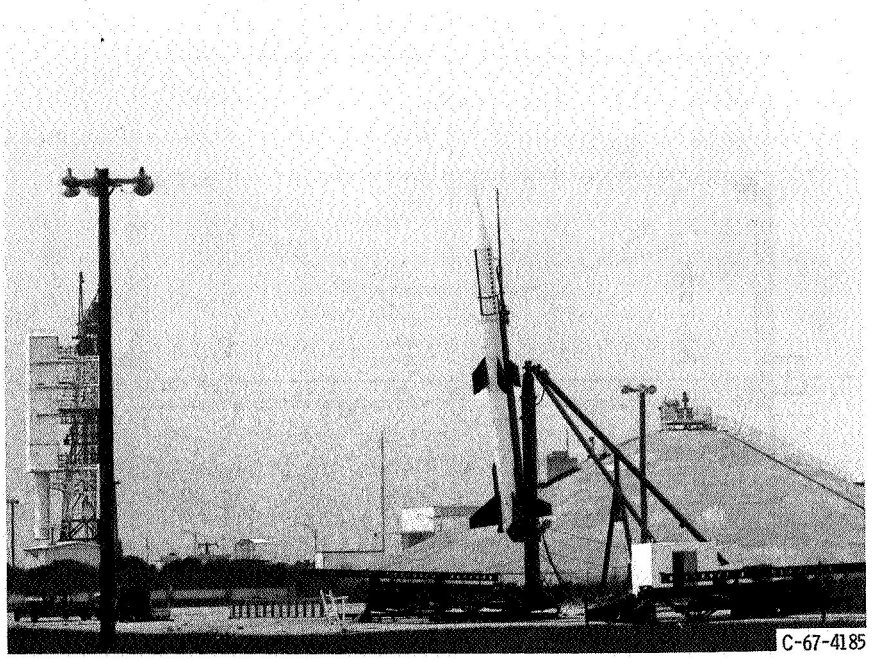

Figure 2. - WASP sounding rocket on launcher.

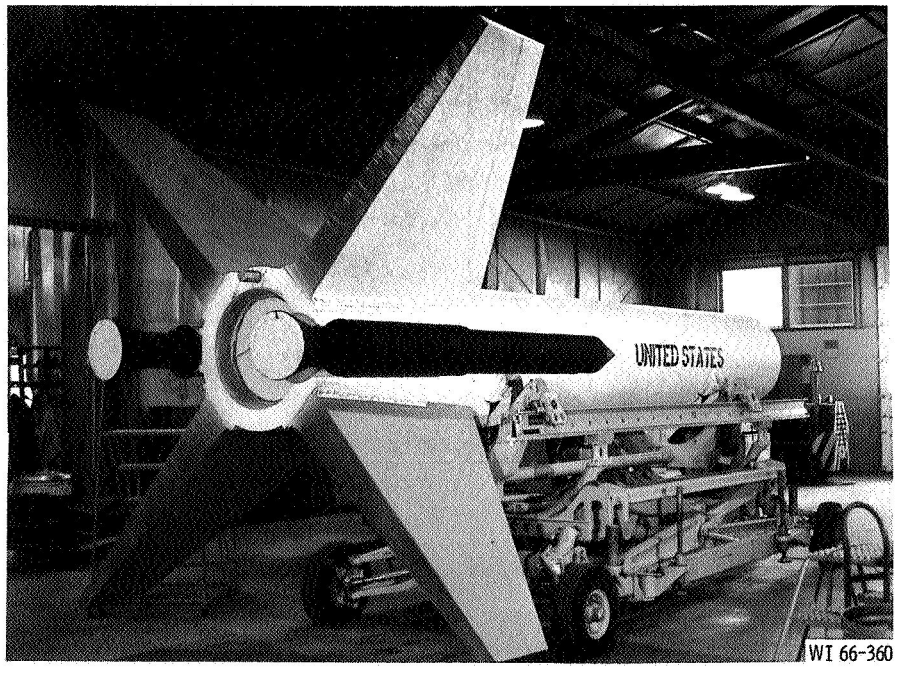

Figure 3. - Assembled first stage.

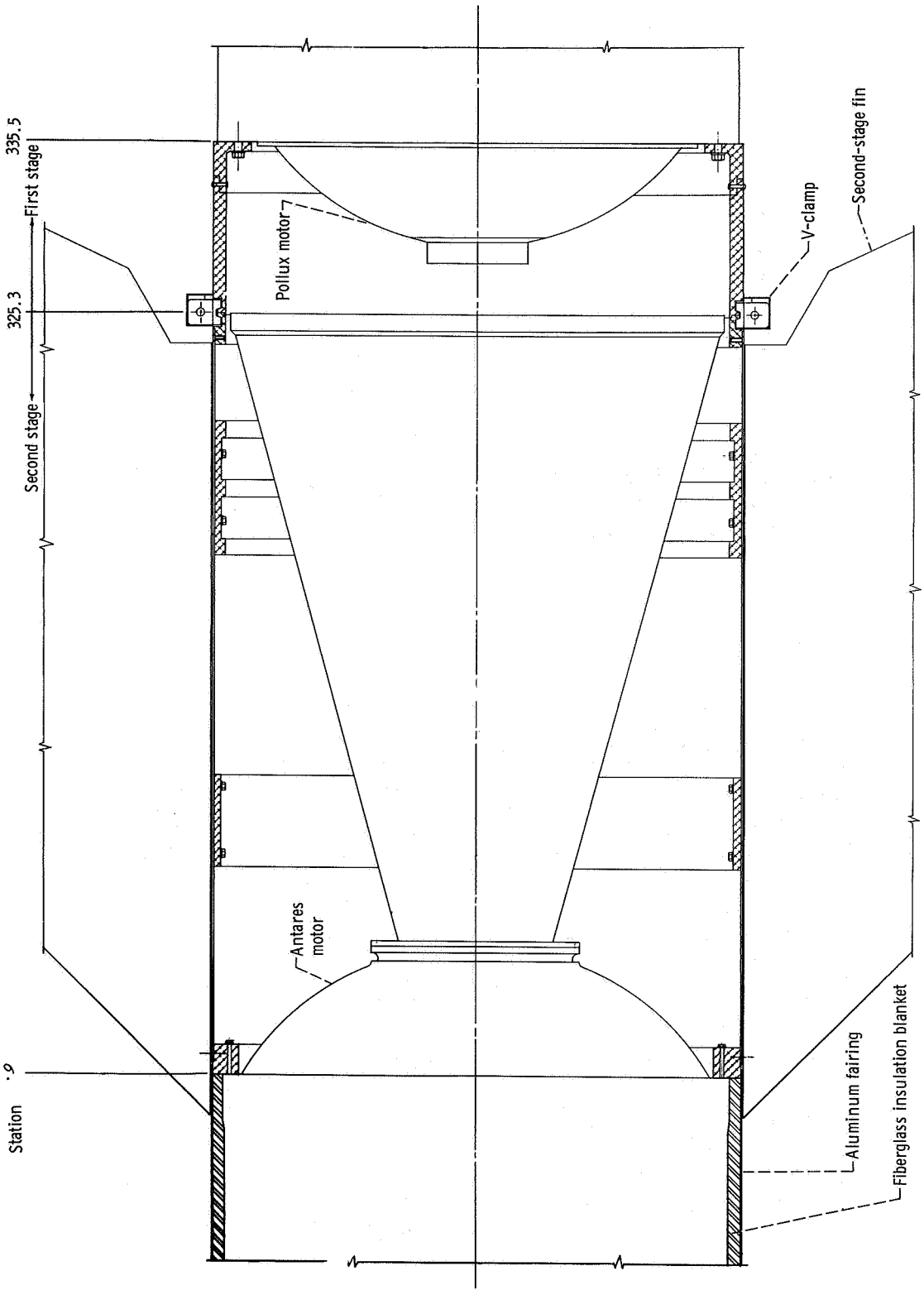

Figure 4. - First- to second-stage interstage structure.

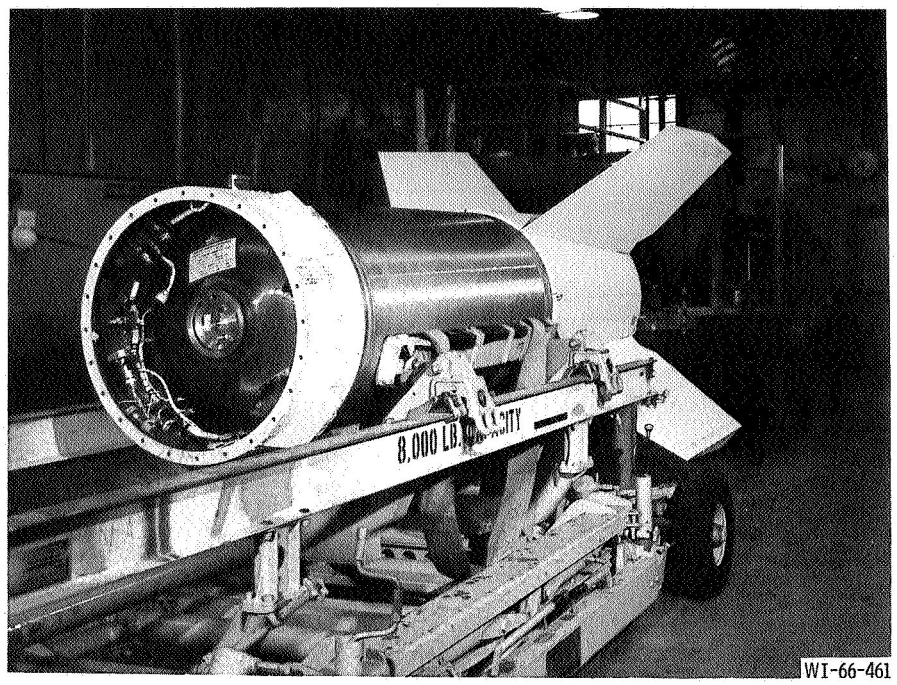

(a) Front view.

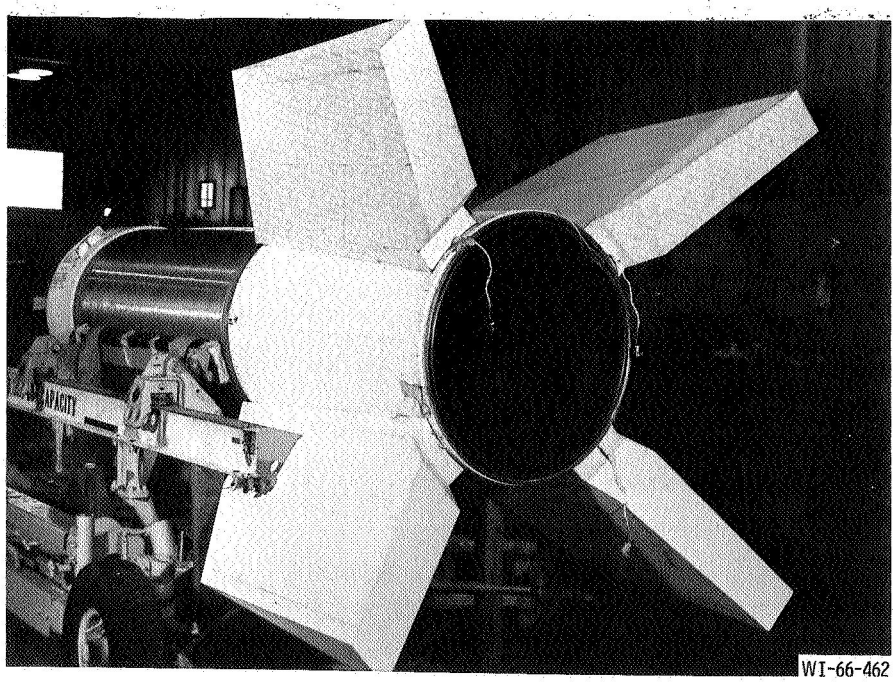

(b) Aft view.

Figure 5. - Assembled second stage without fiberglass insulation blanket and fairing.

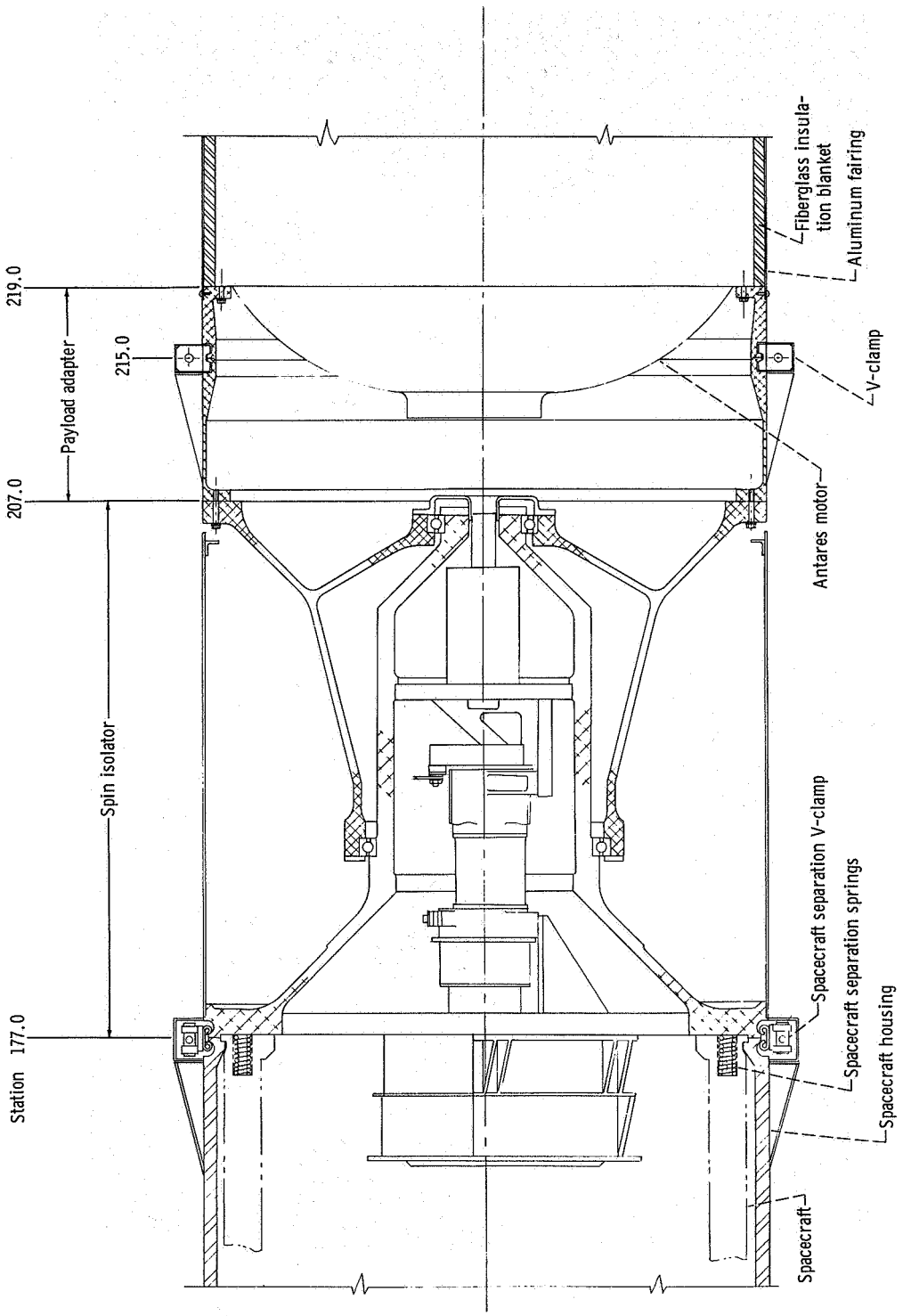

Figure 6. - Second stage to payload interstage structure with spin isolator.

aration joint was not required for this flight as spacecraft separation occurred at station 177. Spacecraft and spacecraft housing separation was accomplished by detonation of the explosive bolts in the four-segment marmon clamp at station 177. The separation force was provided by four helical springs (see fig. 6) assembled in a compressed state into the base of the payload. Each spring had a spring rate of 120 pounds per inch (2140 kg/m) and a travel of 1.75 inches (0.0445 m). This gave a calculated differential velocity of 2.7 feet per second (0.823 m/sec^2) between the spacecraft and spacecraft housing and the spent second stage with spin isolator attached.

Spacecraft housing. - The WASP spacecraft housing including some joint construction details are shown in figure 7. The spacecraft housing consists of three major subassemblies: a conical section 76 inches (1.93 m) long and 31.5 inches (0.8 m) in base diameter, a cylindrical section 82 inches (2.08 m) long and 31.5 inches (0.8 m) in diameter, and a 36-pound stainless-steel ballast conical section 18 inches (0.457 m) long that attaches to the forward end of the conical section. The sting supporting the angle-of-attack transducer was mounted on this ballast section. The conical and cylindrical sections were of similar sandwich-type construction with 0.030-inch-thick (0.8-mm-thick) fiberglass face sheets and 0.560-inch-thick (14.2-mm-thick) fiberglass honeycomb core. The cylindrical section differed in that the face sheets tapered from 0.090-inch (2.4-mm) thickness at station 177 to 0.030-inch (0.8-mm) thickness at station 94.5. Aluminum reinforcing rings are installed at each end of the cylinder and at the base and top of the cone. The cone and cylinder are joined together by radial screws at station 94.5. The spacecraft housing bears against the spacecraft structure through four pads located at both stations 96 and 26.

The heat protection on the housing cone was a commercial ablation material 0.060 inch (1.5 mm) thick applied uniformly to the outside surface of the cone. No heat protection was required on the cylinder. To allow for venting of the honeycomb core, 1/32-inch-diameter (0.8-mm-diam.) holes were drilled in a $1\frac{1}{4}$-inch-square (31.8-mm) pattern over the inner surface of the spacecraft housing.

The ejection mechanism for the spacecraft housing consists of frangible fiberglass blocks (located 180° apart on the housing) which run from the base ring of the cylindrical section to the base of the ballast weight in the nose. A single length of primacord containing 2.13 grams of RDX explosive per meter is installed through the longitudinal hole in the frangible blocks. The spacecraft housing is ejected by initiating the primacord on both ends; the explosion splits the frangible blocks, and the spacecraft housing is split into two 180° shells approximately 177 inches (4.5 m) long, with the sting and ballast assembly remaining attached to one half. Figure 7 shows the split line. The gas generated by the primacord gives the spacecraft housing halves a calculated minimum separation velocity of 8 feet per second (2.44 m/sec).

Pyrotechnic electrical system. - The ignition of the first stage was accomplished by a ground firing system. The Pollux motor was ignited, and first motion breakwires allowed firing of the Recruit motors.

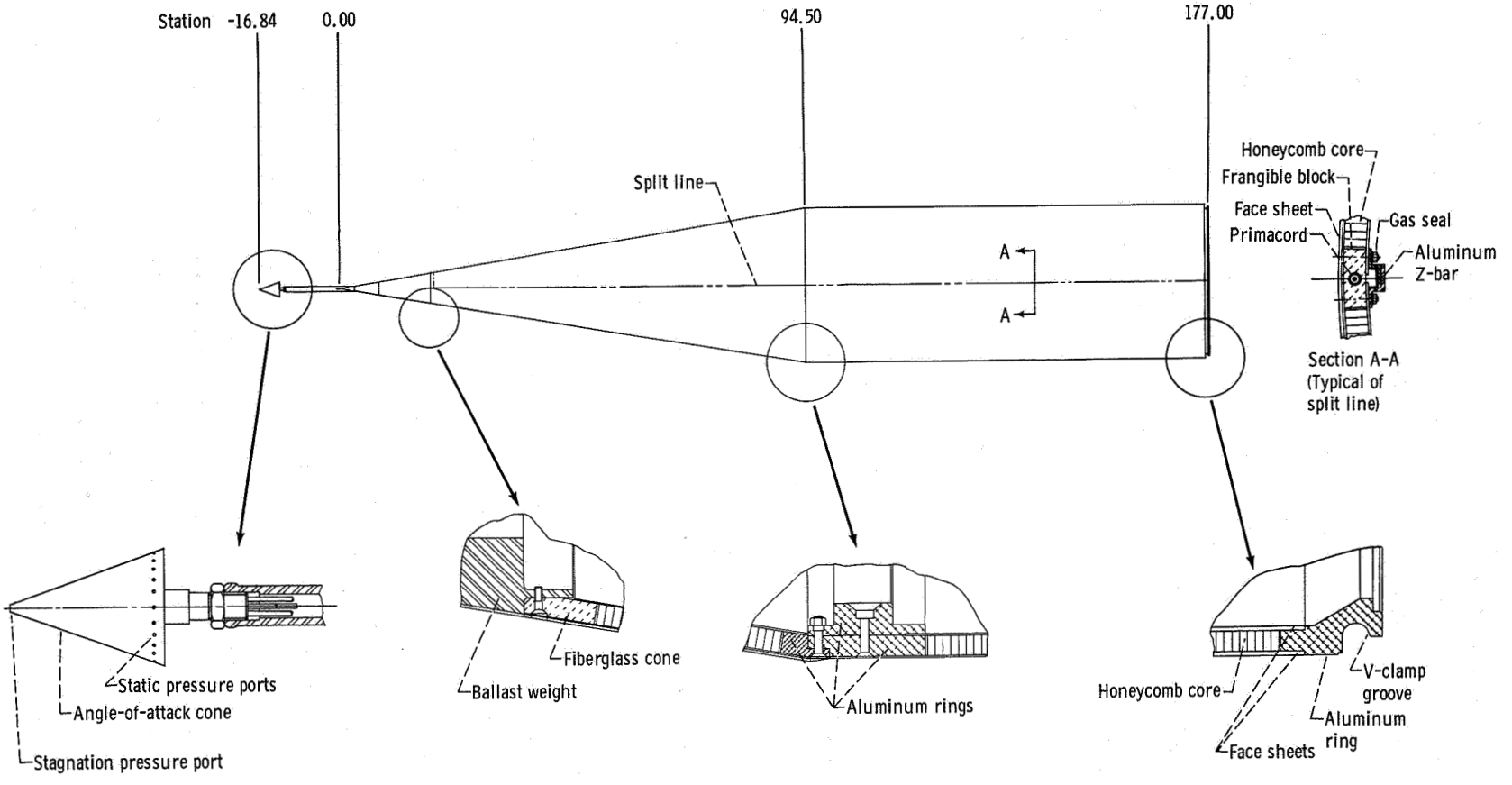

Figure 7. - Spacecraft housing.

Stage separation and ignition of the second-stage motor was initiated by a pair of redundant "g-activated" timers, and power was supplied by redundant remotely activated batteries which were activated on the ground shortly before liftoff. The staging and second-stage ignition circuitry was self-contained in the vehicle and was independent of the spacecraft.

The signal for spacecraft separation and spacecraft housing ejection was provided by a timer in the payload and backed up by the command receiver link of the payload. Power for these two pyrotechnic functions was supplied by redundant batteries of the same type used for second-stage ignition.

Physical and Aerodynamic Data

Mass data. - The calculated time histories of the vehicle weight, center of gravity, roll moment of inertia, and transverse moment of inertia are given in figures 8 to 11. The calculated values are based on measured and manufacturer-provided time histories of the weight, center of gravity, and moments of inertia of the rocket motors, sounding rocket hardware, and payload. In addition, the weight and center of gravity of each of the completely assembled vehicle stages were measured as indicated in figures 8 and 9. The calculated weight and center of gravity of the sounding rocket stages for various times in the trajectory are also given in table I.

TABLE I. - WEIGHT AND CENTER-OF-GRAVITY DATA

Item	Measured weight		Longitudinal center of gravity (distance aft of station 0.0)	
	lb	kg	in.	m
Spacecraft (less housing, arms in)	861.5	392	110.03	2.80
Spacecraft housing (with sting)	287.0	126	111.14	2.82
Spin isolator	379.5	172.1	187.84	4.76
Gross payload	1 528.0	694	129.56	3.29
Second-stage inert	687.0	312	281.84	7.15
Gross at second-stage burnout	2 215.0	1005	176.80	4.49
Second-stage propellant	2 590.0	1177	247.76	6.29
Gross at second-stage ignition	4 805.0	2180	215.05	5.45
First-stage inert[a]	2 601.8	1180	498.05	12.61
Gross at first-stage burnout	7 406.8	3360	314.46	8.0
First-stage propellant[b]	7 680.5	3530	438.02	11.11
Gross at first-stage ignition	15 087.3	6850	375.27	9.53

[a]Includes two Recruit motor casings.

[b]Includes propellant of two Recruits.

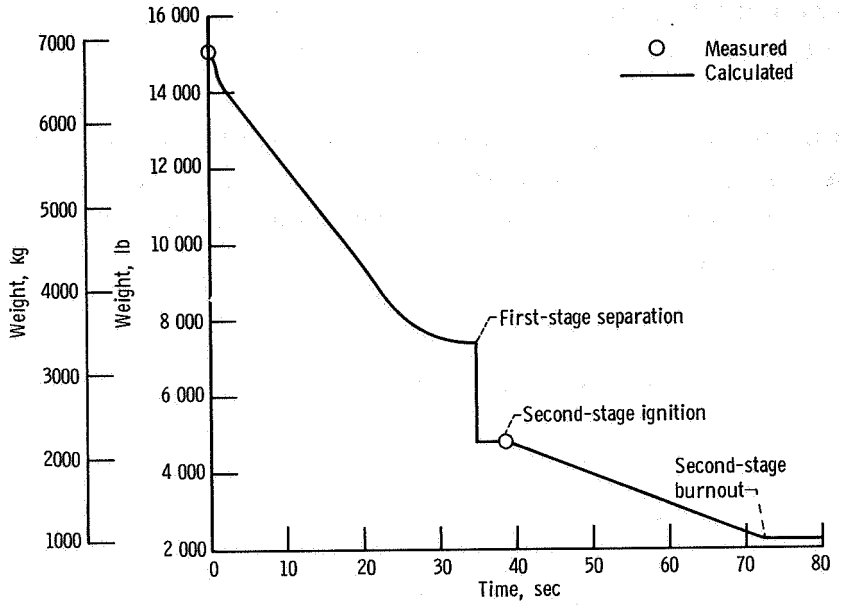

Figure 8. - Time variation of weight.

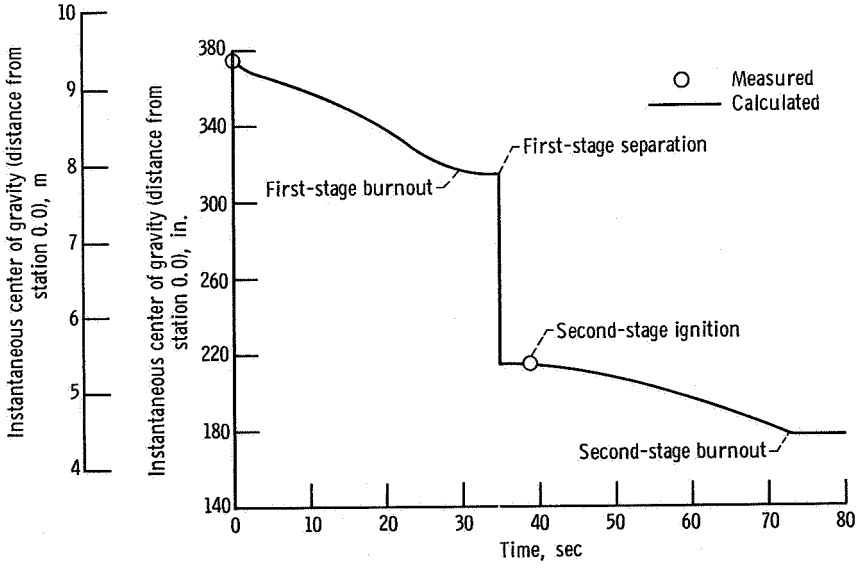

Figure 9. - Time variation of center-of-gravity location.

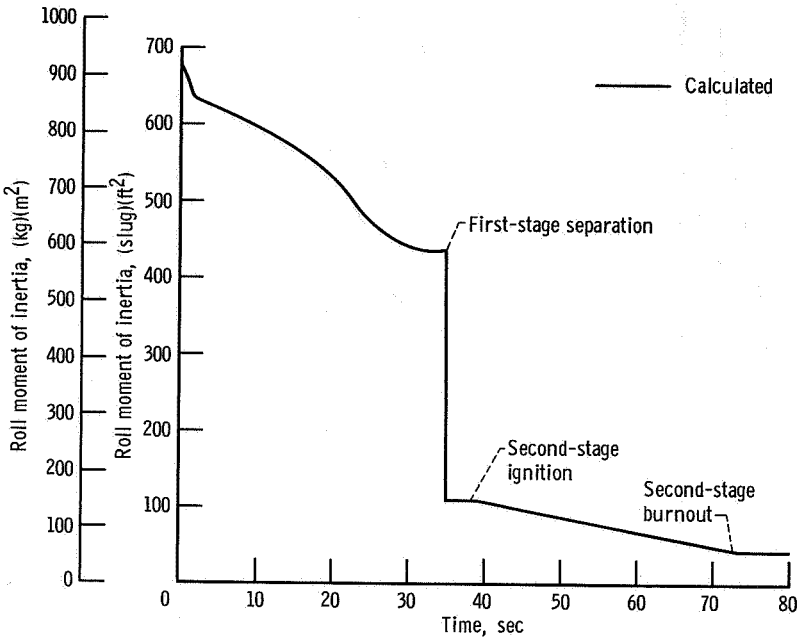

Figure 10. - Time variation of roll moment of inertia.

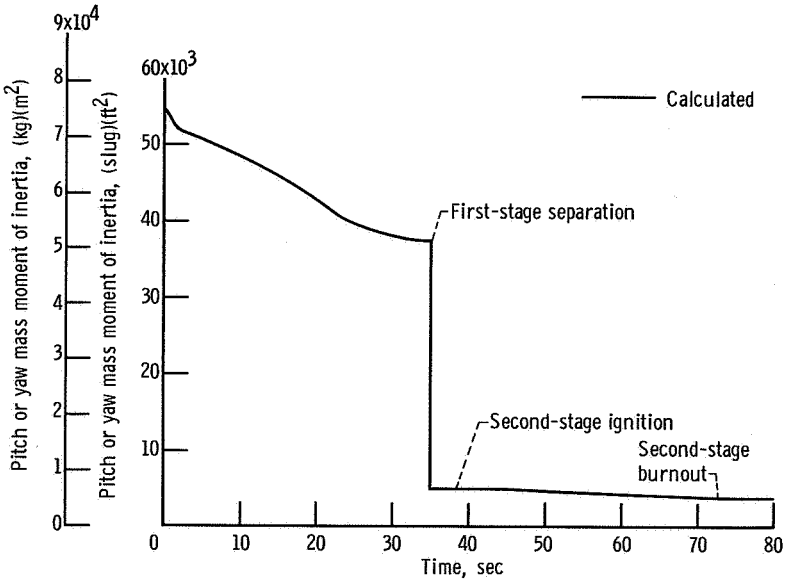

Figure 11. - Time variation of transverse mass moment of inertia.

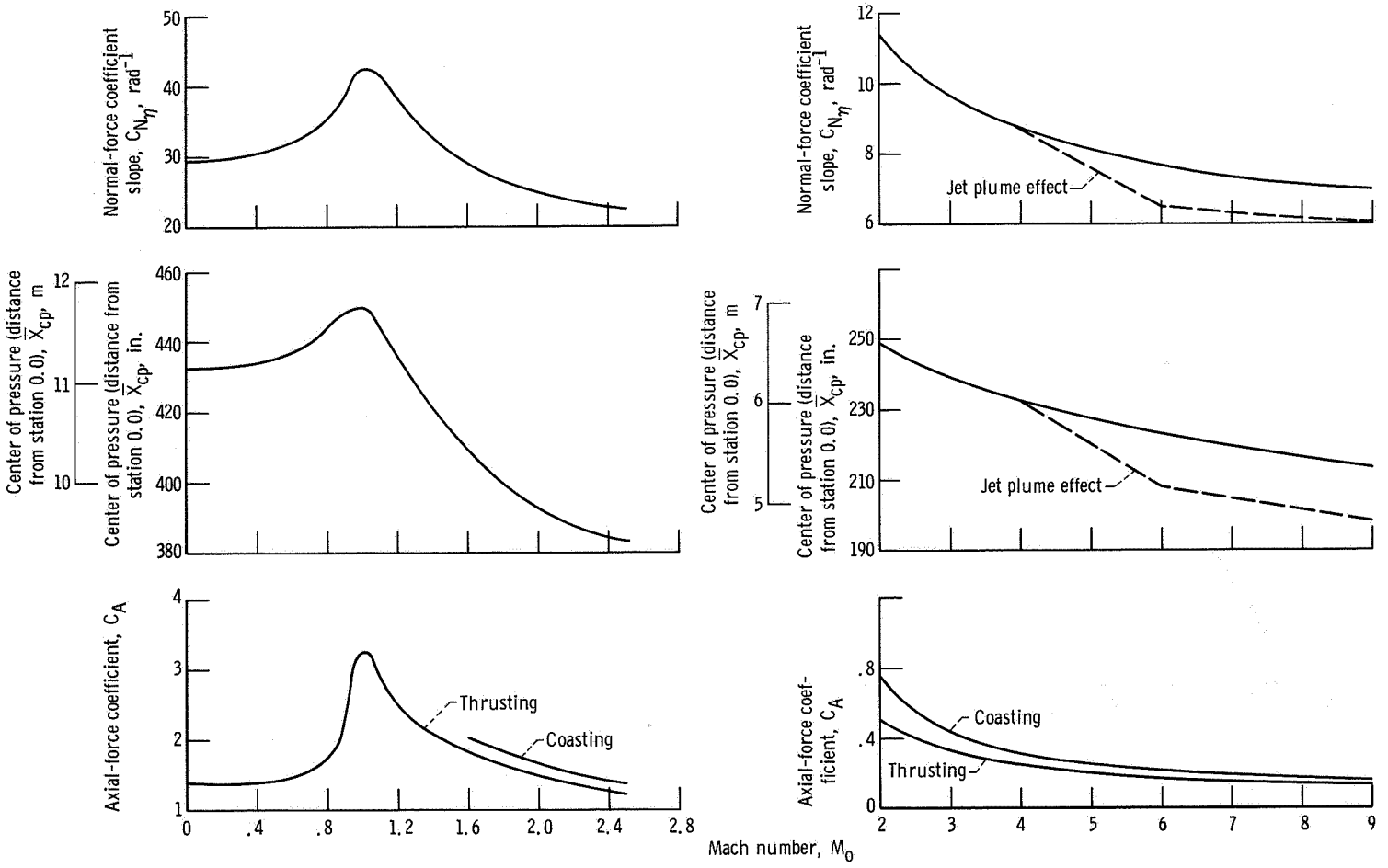

(a) First stage.

(b) Second stage.

Figure 12. - WASP sounding rocket longitudinal aerodynamic characteristics.

Aerodynamic data. - The longitudinal aerodynamic characteristics, normal-force coefficient slope, center of pressure, and axial-force coefficient of the various sounding rocket stages as a function of Mach number are presented in figure 12. The first-stage longitudinal aerodynamic characteristics (fig. 12(a)) were calculated using the method of reference 2, and the results of some limited transonic wind tunnel tests. The second-stage longitudinal aerodynamic characteristics (fig. 12(b)) were based on the results of the wind tunnel test (ref. 3) and calculated cone-cylinder values.

The normal-force coefficient slope and center of pressure curves were modified to account for the loss of effectiveness of stabilizing surfaces at high altitudes in the hypersonic flight regime resulting from the flow separation due to the interference from the rocket exhaust plume. This effect is discussed in reference 4. The data on jet plume effects are limited, and no method for calculating the loss in effectiveness of the second-stage fins was known. Therefore, a conservative estimate of the percent loss in fin effectiveness was made for this configuration when the Mach number was greater than four.

After discussion with the authors of reference 4, it was concluded that the jet plume could induce flow separation when the ratio of jet-exit to free-stream static pressure is greater than 100, which occurs at Mach 6 for the nominal WASP sounding rocket trajectory. The estimated 25 percent loss in effectiveness is based on the percent of fin area that could be in the separated flow region.

The calculated static-stability margin for all sounding rocket stages is presented in figure 13 as center-of-pressure and center-of-gravity variation with flight time. The minimum static margin was 57 inches (1.45 m) during first-stage flight and 19 inches (0.483 m) during second-stage flight. An aeroelastic analysis has shown an additional

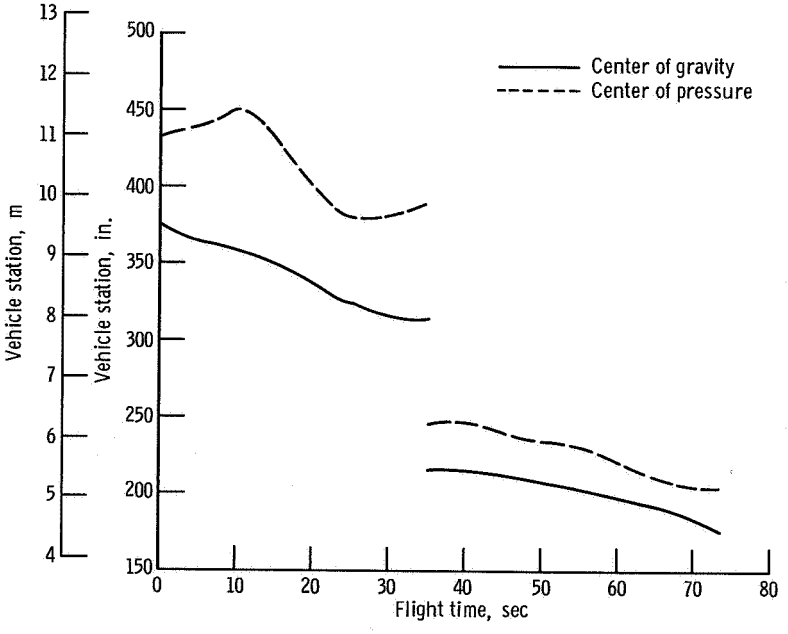

Figure 13. - Calculated static stability margin history.

decrease in the minimum static margin of 2 inches (50.8 mm) during first-stage flight and 3 inches (76 mm) during second-stage flight.

TRAJECTORY PROGRAMMING

Trajectory Calculations

The nominal trajectory parameters presented in this report were calculated by using the Lewis Research Center six-degree-of-freedom trajectory simulation program with an oblate rotating earth. The trajectory simulation program utilizes a 7094 digital computer to solve Euler's differential equations of motion with six degrees of freedom by the fourth-order Runge-Kutta method. Data inputs to the trajectory simulation program include vehicle physical and aerodynamic characteristics, thrust, various misalinements, fin cant angles, and winds.

Wind Compensation

Winds at the time of launch are a major cause of perturbations on the trajectory of an unguided rocket vehicle. Conducting a safe rocket flight about the nominal trajectory necessitates compensation for wind velocity and direction by adjusting the launcher elevation and azimuth about the nominal values at launch time. The wind compensation technique of reference 5 was utilized to obtain the wind correction launcher settings. The accuracy of this method is dependent upon ability to measure launch wind and to predict the vehicle's response to that wind.

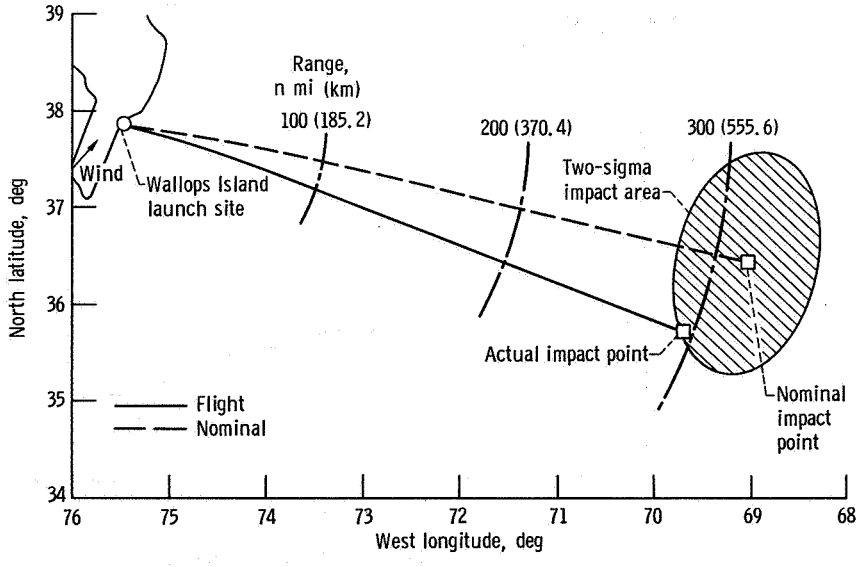

Figure 14. - Plan view of trajectory showing two-sigma dispersion area.

Dispersion Analysis

A dispersion analysis was performed in order to estimate the one-, two-, and three-sigma limits of the payload impact area. Impact dispersions were computed using the simulation perturbation on the nominal no-wind trajectory. The perturbations accounted for in the dispersion analysis included aerodynamic misalinements, dynamic unbalance, wind malassessment, tipoff rates during staging, weight malassessment, change in impulse, thrust misalinement, launcher setting errors, and timing errors in staging and second-stage ignition. The total dispersion was obtained by taking the square root of the sum of the squares of the effects of the individual perturbations. Figure 14 is a plan view of the trajectory showing the two-sigma dispersion area around the nominal impact point.

CAPABILITIES

Since WASP sounding rocket is a new vehicle configuration, the calculated capabilities of the WASP sounding rocket are presented for information in table II. The capabilities presented are based upon no-wind trajectory calculations for 80° launch elevation and 103° azimuth from Wallops Island, Virginia.

TABLE II. - WASP SOUNDING ROCKET CAPABILITY

[Elevation, 80° (no wind); azimuth, 103° (from Wallops Island, Virginia).]

Parameter	Payload weight, lb (kg)[a]		
	1000 (454)	1250 (577)	1528 (694)
Apogee, n mi (km)	234 (415)	170 (315.5)	140 (260)
Apogee time, sec	368	316	288
Total range, n mi (km)	445 (825)	374 (694)	320 (535)
Peak axial load factor, g's	10.78	9.50	8.43
Maximum dynamic pressure, psf (N/m^2)	3500 (167 500)	2853 (136 500)	2772 (132 500)
Time above 250 000 ft (76.25 km), sec	585	471	408
Parameter at second-stage burnout			
Mach number	9.86	7.91	6.98
Spin rate, Hz	3.76	3.88	3.80
Flight path angle in pitch, deg	60.36	56.91	55.39
Altitude, n mi (km)	37.4 (69.4)	32.0 (59.3)	29.9 (55.5)
Range, n mi (km)	18.2 (33.8)	17.2 (31.9)	16.7 (31)
Velocity, ft/sec (m/sec)	9470 (2890)	8331 (2540)	7603 (2320)

[a]Payload weight is defined as total weight forward of station 207.

TELEMETRY AND INSTRUMENTATION

Telemetry System

The flight data for the launch vehicle was transmitted via the spacecraft telemetering system which was of FM/FM type with a carrier frequency of 240.2 megahertz transmitting at a power of 10 watts. Seventeen continuous and one commutated channels were used. Table III summarizes the measurements which were taken in flight. The data telemetered are considered to be accurate within 3 percent.

TABLE III. - SUMMARY OF INSTRUMENTATION

Measurement	Location and orientation		Instrument	Range	Frequency response, Hz
	Station number	Sensing axis (fixed with payload)			
Angle of attack	-15	Pitch	Aerocone	$\pm 20^{\circ}$	10
Angle of attack	-15	Yaw	Aerocone	$\pm 20^{\circ}$	10
Acceleration	87	Thrust	Potentiometer accelerometer	-2 to 15 g's	50
Spin rate	---	Spin isolator	Continuous potentiometer	----------	---
Vibration 1	21	Pitch	Potentiometer accelerometer	±20 g	50
Vibration 2	94.5	Yaw	Potentiometer accelerometer	±20 g	50
Vibration 3	175.5	Yaw	Potentiometer accelerometer	±20 g	50
Vibration 4	175.5	Pitch	Potentiometer accelerometer	±20 g	50
Vibration 5	94.5	Thrust	Piezoelectric accelerometer	±20 g	600
Vibration 6	175.5	Thrust	Piezoelectric accelerometer	±20 g	790
Vibration 7	95	Pitch	Piezoelectric accelerometer	±20 g	1050
Chamber pressure	-----	First stage	Potentiometer transducer	0 to 700 psi (0 to 4 825 000 N/m^2)	Commutated
Chamber pressure	-----	Second stage	Potentiometer transducer	0 to 700 psi (0 to 4 825 000 N/m^2)	Commutated
Cone static pressure	-----	Sting	Potentiometer transducer	0 to 30 psi (0 to 207 000 N/m^2)	Commutated
Total pressure	-----	Sting	Potentiometer transducer	0 to 50 psi (0 to 345 000 N/m^2)	Commutated
Low-level acceleration	46	Thrust	Servo rebalance accelerometer	±0.001 g ±0.01 g	Commutated Commutated
Vehicle rate	58	Pitch	Rate gyro	$\pm 3.6^{\circ}$/sec	6
Vehicle rate	58	Yaw	Rate gyro	$\pm 3.6^{\circ}$/sec	8
Payload rate[a]	58	Roll	Rate gyro	$\pm 3.6^{\circ}$/sec	11
Vehicle position	40	Pitch[b]	Magnetometer	±0.6 G (0.00006 tesla)	10
Vehicle position	40	Yaw[b]	Magnetometer	±0.6 G (0.00006 tesla)	10
Payload position[a]	40	Roll[b]	Magnetometer	±0.6 G (0.00006 tesla)	10

[a]Roll rate and position measured were of nonspinning payload and not of spinning vehicle.

[b]Indicates sensor centerline direction; readings change due to position changes in other two orthogonal planes.

Instrumentation

Angle of attack. - The pitch and yaw angles of attack were measured with a transducer mounted on a sting (fig. 1) which positioned the transducer about 16 inches (0.4 m) forward of station 0.0. The transducer consisted of a 20° half-angle cone, 3.0 inches (76 mm) in diameter at the base, supported at the center of gravity but free to rotate in two perpendicular planes. The relative motion between the cone and the sting was measured by two linear potentiometers. The transducer was capable of measuring $\pm 20^{\circ}$ in pitch and yaw with a $\pm 0.1^{\circ}$ resolution in a Mach number range of 0 to 10 and an altitude range of sea level to 100 000 feet (30.5 km). It was also capable of operating at a temperature of 1000° F (810° K).

Dynamic pressure. - The angle of attack transducer described previously had a stagnation pressure port at the tip and cone static pressure ports around the circumference of the cone surface near the base. The stagnation and static ports were connected to two potentiometer-type pressure transducers, 0- to 30-pound-per-square-inch-absolute (207 000-N/m^2) range for static pressure and 0- to 50-pound-per-square-inch absolute (345 000-N/m^2) range for stagnation pressure.

Spin rate. - The method used to obtain spin rate was unique as it took advantage of the condition that this spinning vehicle had a nonspinning payload. Reference 1 shows that the payload spin rate was negligible. A continuous potentiometer was installed on the centerline at the base of the payload, so that the case of the potentiometer was fixed on the spinning part while the shaft was stationary with the payload. This gave a continuous indication of angular position with time, and the number of revolutions per unit time yields spin rate.

Longitudinal load factor. - Longitudinal acceleration was measured with a conventional potentiometer type accelerometer of -2- to 15-g range mounted on the spacecraft with the sensitive axis in the thrust direction.

Motor thrust. - The pressure in the Pollux and Antares motors was measured with conventional potentiometer-type pressure transducers with 0- to 700-pound-per-square-inch-absolute (4 825 000-N/m^2) range. Thrust was calculated from pressure using the pressure data and the known thrust coefficients of the nozzles.

Vibration. - Two types of vibration measuring instruments having ±20-g range were used. Four were potentiometer-type instruments and three were piezoelectric devices. The locations of these units and their axis orientations are given in table III.

Trajectory. - Flight altitude, range, and velocity information was obtained from the radar data supplied by Wallops Station. The vehicle was skin tracked by the FPQ-6 and FPS-16 radars at Wallops Station.

RESULTS AND DISCUSSION

Vehicle Trajectory

The nominal launcher settings at NASA Wallops Station were an elevation of 80° and an azimuth of 103° East of true North. The actual launcher settings were 77.7° elevation and 85° azimuth to compensate for existing winds at the time of launch. The ballistic wind was 21.8 feet per second (6.65 m/sec) from an azimuth of 224.8°. The sequence of trajectory events is presented in table IV. The total vehicle weight was 15 087 pounds (6 850 kg) at launch and the initial acceleration was approximately 10 g's.

TABLE IV. - SEQUENCE OF TRAJECTORY EVENTS

Item	Time, sec	
	Nominal	Actual
First-stage ignition	0.0	0.0
Recruit ignition	.14	.16
Recruit burnout	2.40	(a)
First-stage burnout	34.0	(b)
First- to second-stage separation	35.0	35.0
Second-stage ignition	38.7	38.5
Second-stage burnout	72.7	[c]76.0
Spacecraft separation	95.0	95.0
Spacecraft housing ejection	97.0	97.0
Apogee	288.0	286.0
Impact	632	(d)

[a]No instrumentation available.
[b]Separation occurred before thrust decayed to zero.
[c]Thrust was zero pounds as indicated by pressure transducer. See the section Residual burning in text.
[d]Could not be obtained from radar data.

Recruit ignition occurred at 0.16 second after Pollux ignition. First-stage burnout occurred at approximately 35 seconds (nominal burnout time is 34 sec). Stage separation occurred at 35 seconds, and second-stage ignition occurred at 38.5 seconds (nominal ignition time is 38.7 sec). Second-stage burnout occurred at 76 seconds.

Figure 15 shows comparison of actual and expected altitude-range plot. The actual data were obtained from the FPQ-6 and FPS-16 radars at Wallops Station. The apogee altitude was 6 nautical miles (11.1 km) or 4.3 percent low of the predicted altitude, and the range was 25 nautical miles (46.3 km) or 7.8 percent short of the predicted range. The actual impact point was 41 nautical miles (76 km) from the predicted impact point and within the two-sigma dispersion area as shown in figure 14.

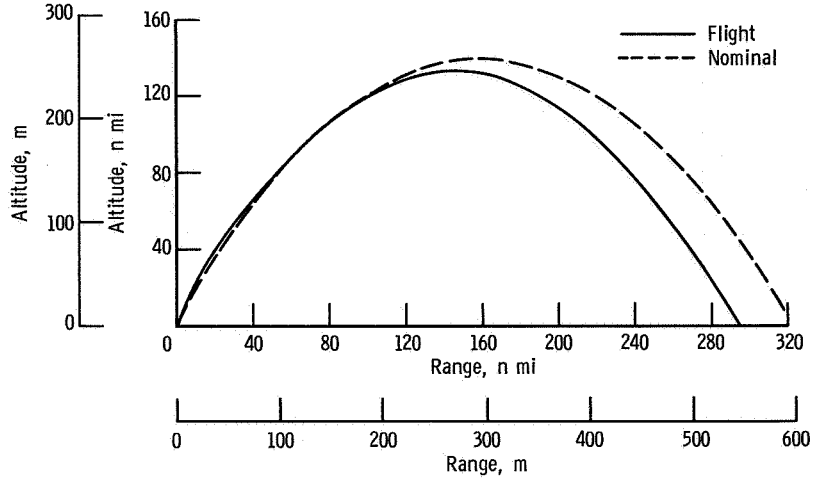

Figure 15. - WASP sounding rocket altitude-range plot.

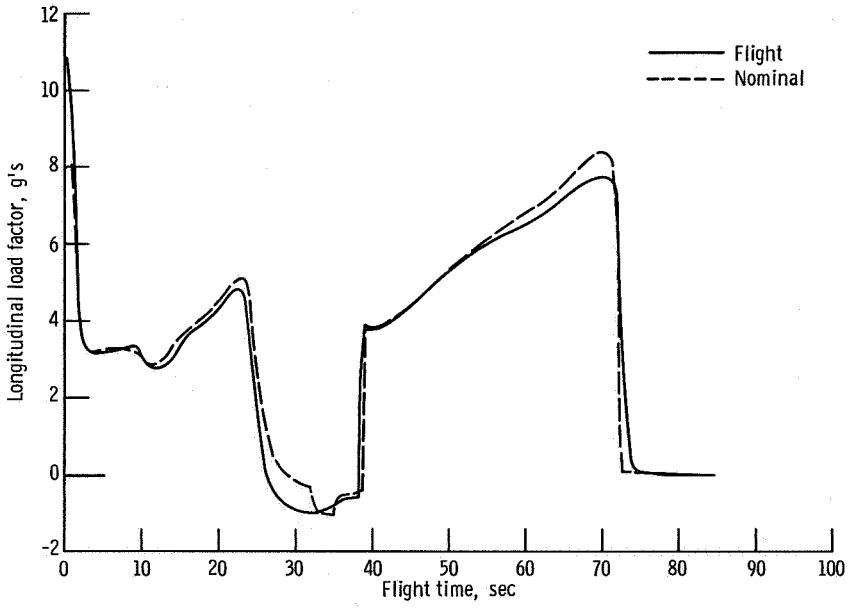

Figure 16. - Longitudinal load factor history.

Vehicle Performance

The longitudinal load factor history is presented in figure 16 and compared to the nominal factor. At lift-off, the longitudinal load factor was 10.6 g's. After lift-off, the maximum longitudinal load factor during first-stage burning was 4.8 g's. The maximum longitudinal load factor during second-stage burning was 7.7 g's at 70 seconds. Comparisons of the actual and nominal velocity and Mach number histories are shown in

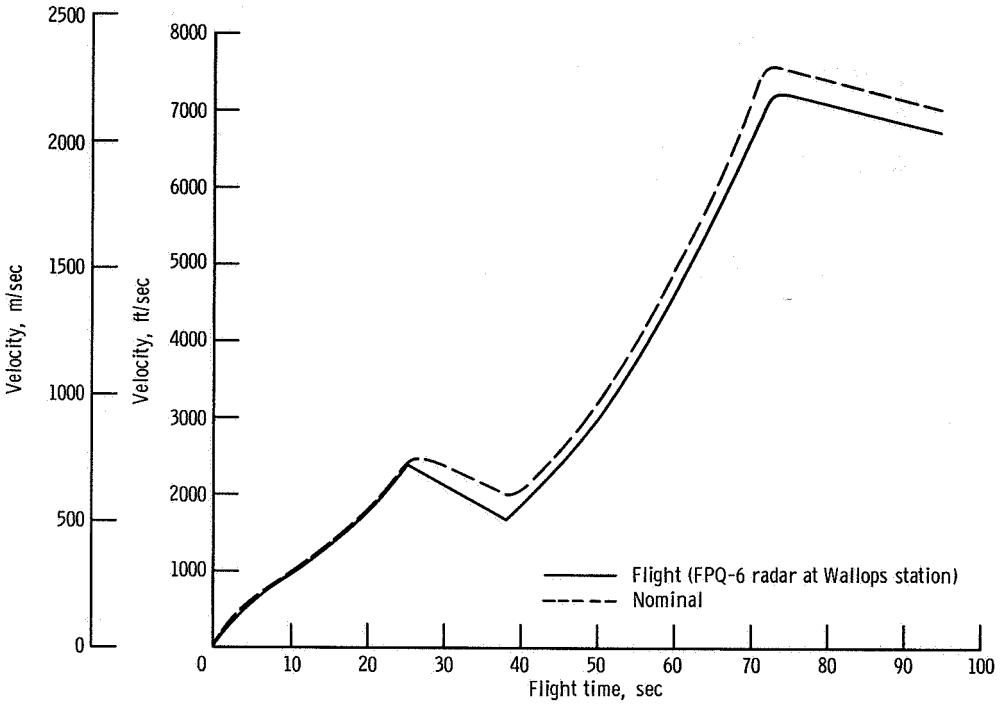

Figure 17. - Velocity history.

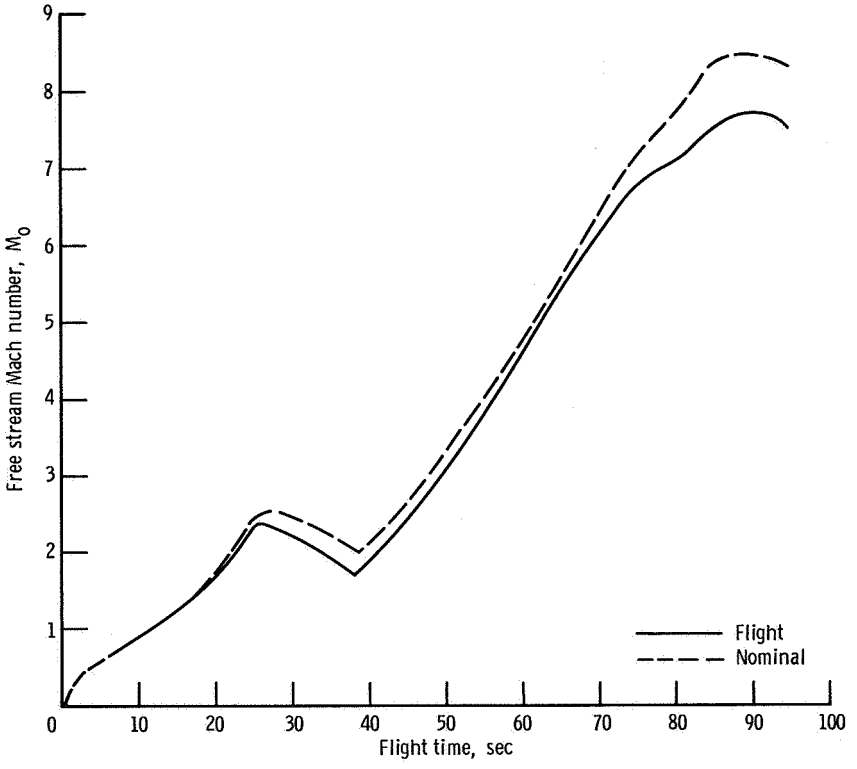

Figure 18. - Mach number history.

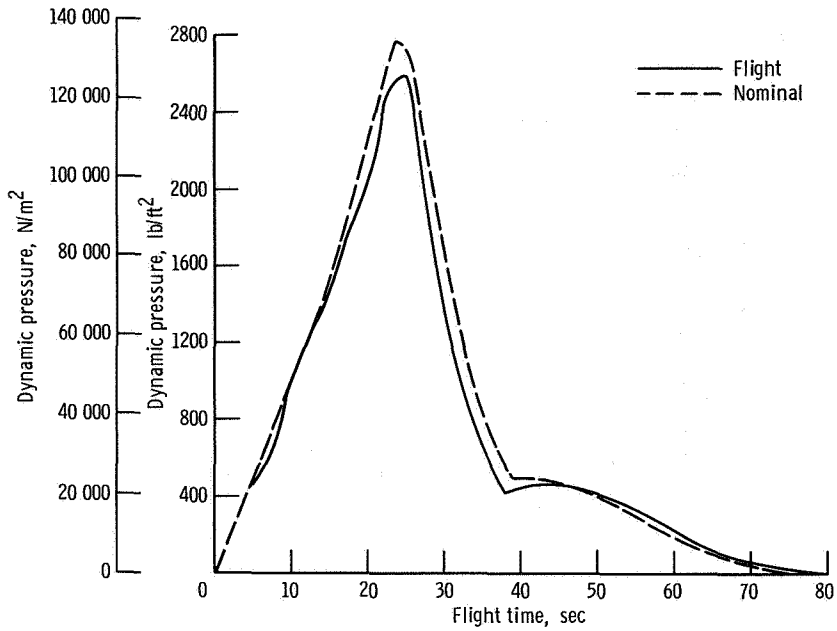

Figure 19. - Dynamic pressure history.

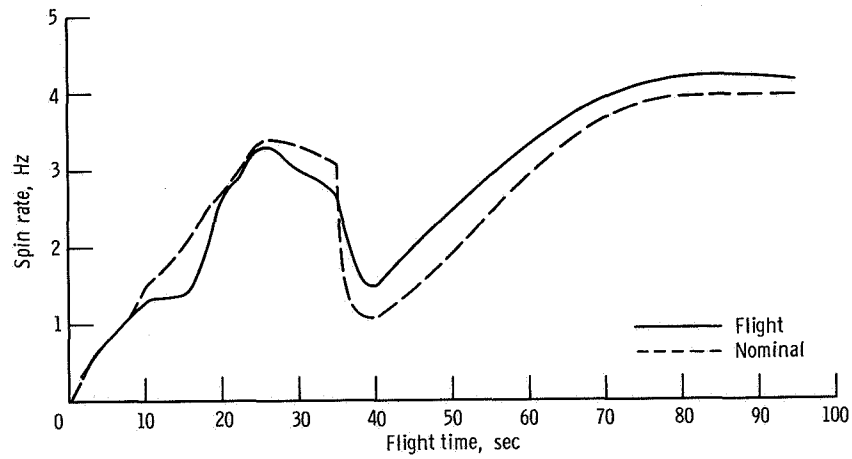

Figure 20. - Spin rate history.

figures 17 and 18. The velocity at second-stage burnout was 400 feet per second (122 m/sec) lower than expected. The dynamic pressure history calculated from radar data and reference 6 is shown in figure 19. The maximum dynamic pressure was about 2600 pounds per square foot (124 000 N/m^2) at 25 seconds. The attempt to directly measure dynamic pressure using the pressure ports located on the angle-of-attack transducer (see fig. 7) was unsuccessful because of an instrumentation malfunction.

The spin rate history of the sounding rocket as shown in figure 20 assumes that the payload did not rotate, and reference 1 shows that the payload spin was negligible. The maximum spin rate during first-stage burning was 3.3 hertz at 26 seconds. The spin rate at 85 seconds was 4.22 hertz and was 0.27 hertz higher than predicted.

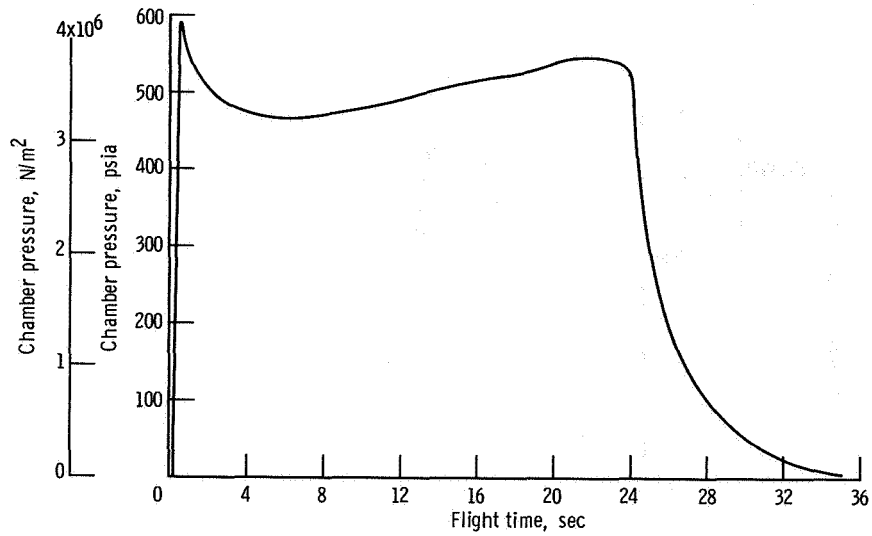

Figure 21. - Pollux motor chamber pressure history.

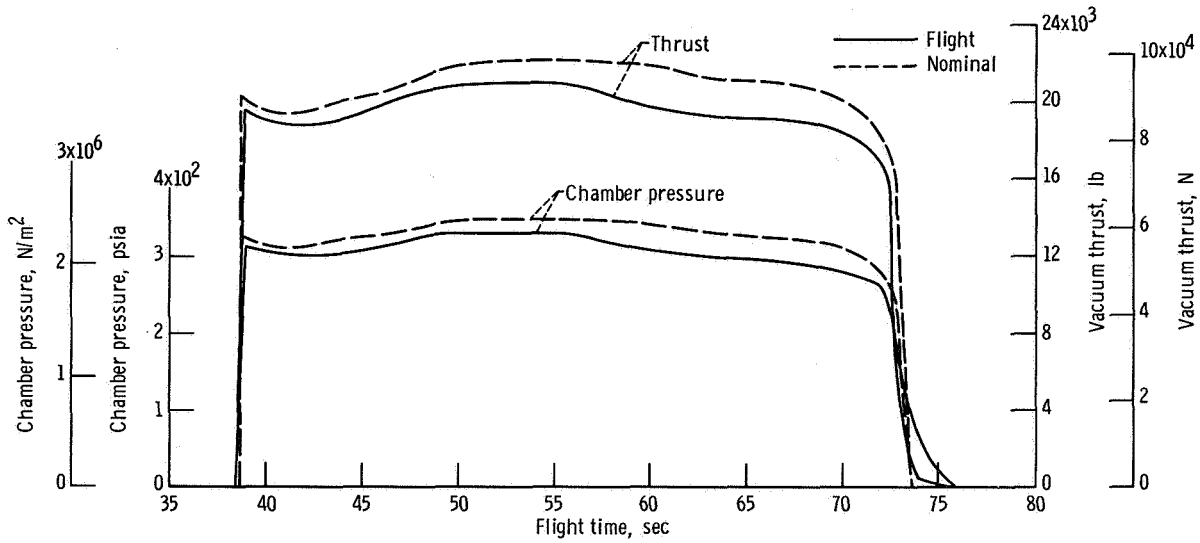

Figure 22. - Antares motor chamber pressure and vacuum thrust history.

Rocket motor performance. - Figures 21 and 22 show the Pollux and Antares stage motor chamber pressure histories as obtained by pressure transducers mounted on the forward end of each motor. The chamber pressure measurements were telemetered on continuous channels. The thrust levels in figures 22 and 23 were derived using the manufacturer's thrust coefficients and nozzle throat areas. The flight thrust levels are compared to nominal motor thrust. The Pollux motor total impulse was 3 percent greater than the nominal value, and the Antares motor total impulse was 5 percent less than the nominal value.

Angle-of-attack history. - Figure 24 shows the α, β, and η histories up to 60 seconds of flight. The angle-of-attack data are presented as qualitative information. The

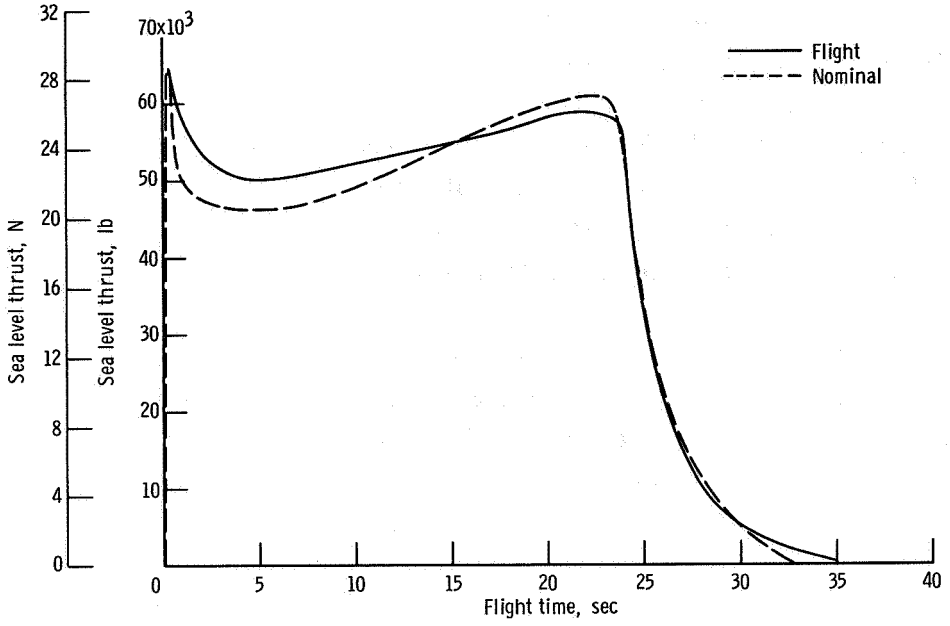

Figure 23. - Pollux motor thrust history.

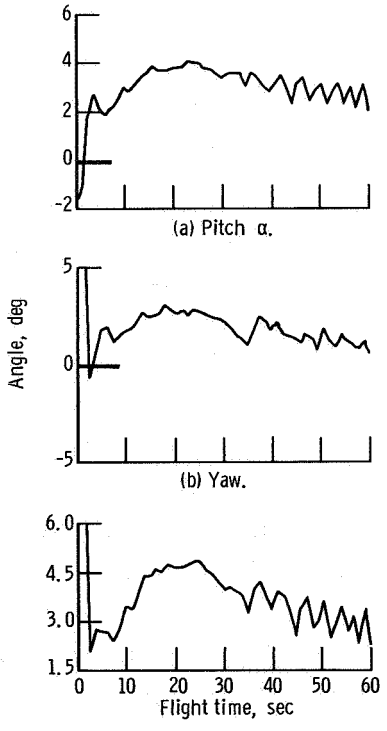

Figure 24. - Angle-of-attack history.

data has not been corrected for angle errors which were estimated at $\pm 1^{o}$ because of misalinement of the transducer and sounding rocket longitudinal axes or for true rotational position relative to the pitch and yaw axes. The data shown in figure 24 indicate that the vehicle had a small coning angle during flight up to 100 000 feet (30.5 km), which is the altitude limit of the transducer. In addition, rate gyros located on the spacecraft indicated that the vehicle started to experience a divergent coning motion at burnout. The available data was insufficient to make an analysis of the post-burnout coning of the vehicle.

Low and short trajectory. - The low and short trajectory may be due to a higher than expected drag during first-stage burn. During the first 15 seconds of flight, the first-stage motor thrust was higher than the nominal thrust (see fig. 23), which compensated for the high drag. Therefore, the velocity during this time nearly matched nominal velocity. During the remainder of first-stage flight, the thrust was near the nominal level, and the higher drag resulted in the velocity being 300 feet per second (91.5 m/sec) low at second-stage ignition (fig. 17). The second-stage thrust was near nominal value during the first 17 seconds of second-stage flight, and the velocity remained 200 to 300 feet per second (61 to 91.5 m/sec) low. During the remainder of second-stage burn, the thrust level was 5 percent low resulting in a 400-feet-per-second (122-m/sec) low velocity at second-stage burnout.

Residual burning. - The Antares motor has a characteristic long thrust decay time because of residual burning. Data available before flight from ground tests and Scout flights showed that in the worst case the thrust level would be zero 56 seconds after ignition. The nominal burning time for the Antares motor is 34 seconds. To minimize the probability of a collision between the separated payload and spent second stage, with spin isolator, the separation time was set for 95 seconds of flight time (56 sec after nominal second-stage ignition). However, signals from spacecraft-rate gyros and accelerometers (ref. 1) indicated that a collision occurred at 104 seconds of flight time. A low-level accelerometer with a maximum range of ± 0.01 g located on the spacecraft indicated a 0.01-g acceleration during the expected residual burning period. There was no indication that the acceleration was decreasing. A thrust level of 22.1 pounds was calculated using the 0.01 g acceleration and the 2215-pound (1000-kg) gross weight of the second-stage and spin isolator. Calculations show that a collision could occur at 103.5 seconds of flight time. These calculations were made assuming the 22.1-pound (98.1-N) constant thrust applied to the 1067-pound (484-kg) second stage with attached spin isolator, a 2.7-foot-per-second (0.825-m/sec) differential separation velocity, no tip-off rates, and a constant 0.007-g forward acceleration was part of the experiment program as described in reference 1. The spacecraft was not damaged by the collision.

Vibration. - The flight vibration environment was measured by potentiometer and piezoelectric accelerometers; the type, station location, and sensitive axes of these instruments are shown in table III. Data from the potentiometer-type accelerometers show

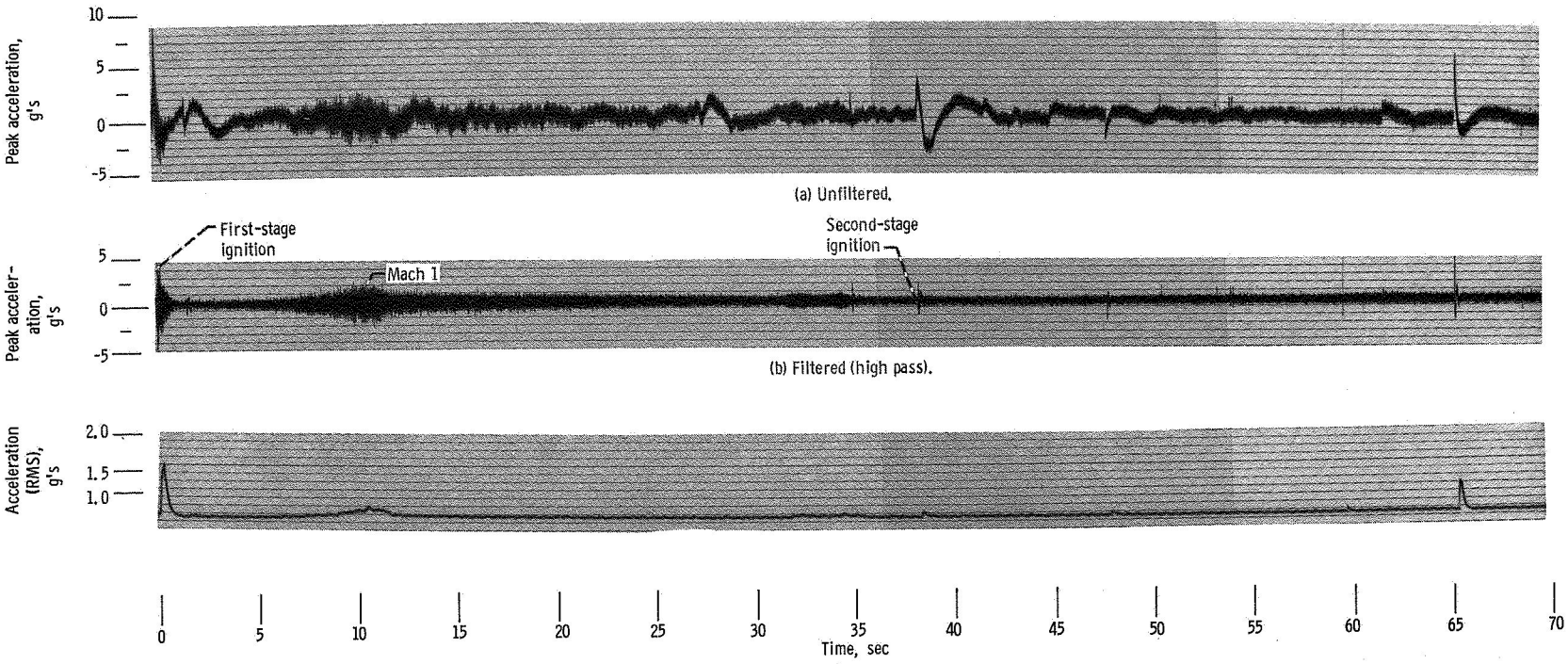

Figure 25. - Variation of thrust-axis vibration from accelerometer number 6 with time.

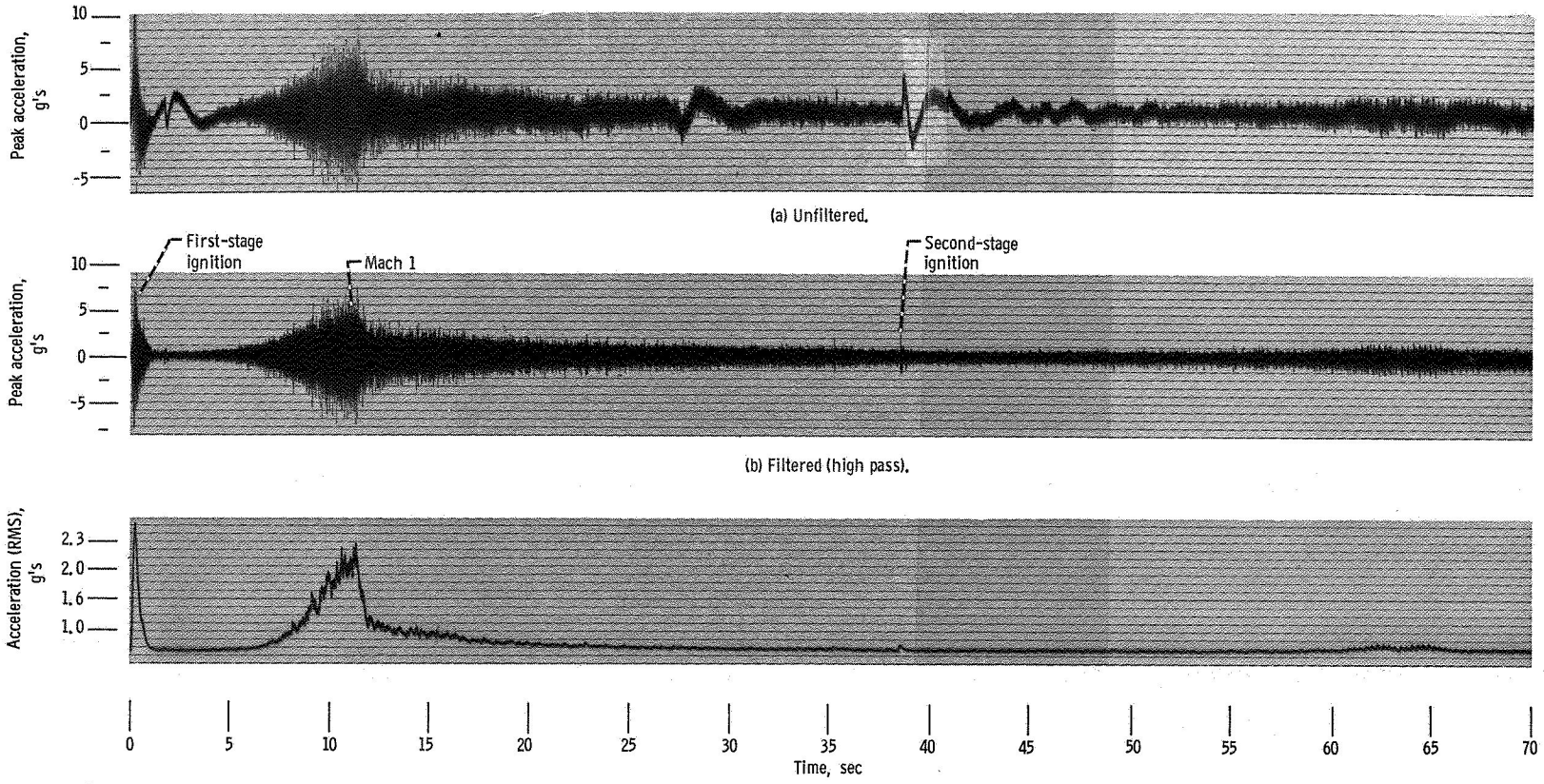

Figure 26. - Variation of thrust-axis vibration from accelerometer number 5 with time.

that the lateral load factors in flight were always less than 1 g. The data as received from piezoelectric accelerometers on the thrust axis are presented in figures 25 and 26.

In order to further define the vibration environment, the piezoelectric data were analyzed for amplitude and frequency. The piezoelectric accelerometer systems used had a flat frequency response above 5 hertz and were susceptible to zero shift from high-amplitude shocks of short duration. To eliminate the effects of zero shift and the unknown low-frequency characteristics, the data were passed through a high pass filter. The corner frequency was set to 5 hertz, and the low-frequency rolloff was 24 decibels per octave. The high-frequency rolloff, 18 decibels per octave, was determined by the telemetry system. The resultant filtered data are more readily understood than the unfiltered data. The flight data were segmented into the most significant areas, and tape loops were made for power spectral density (PSD) and amplitude probability density (APD) analysis. The PSD plots were made using a parallel filter analyzer having a frequency range from 12.5 to 2 000 hertz, and containing 80 filters each with a 25-cycle bandwidth. The standard error of the PSD plot is 15 percent. The RMS levels were measured using a true RMS meter.

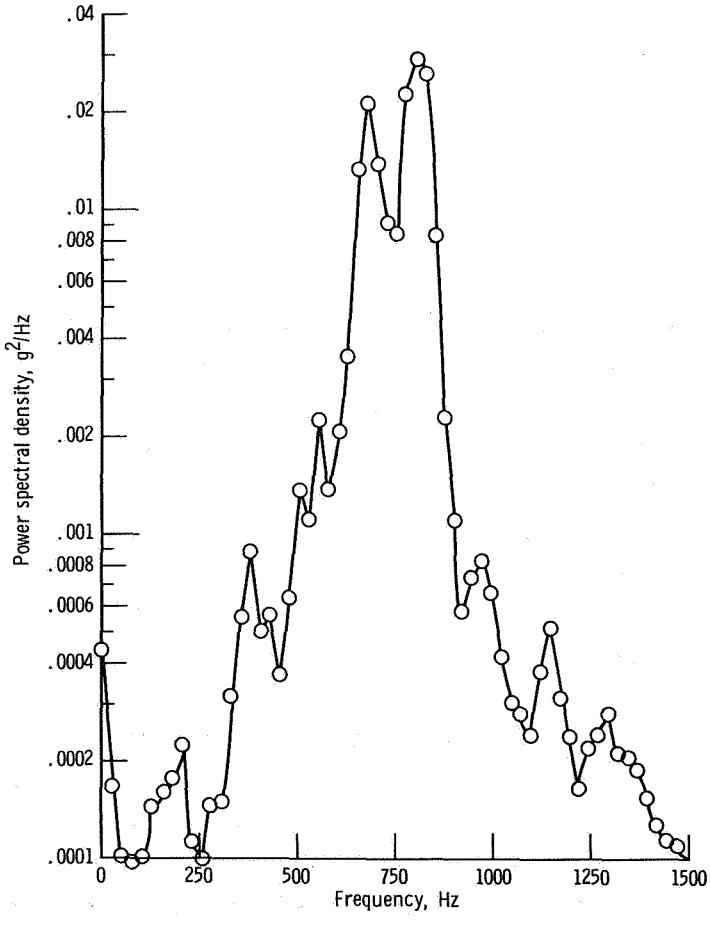

Figure 27. - Power spectral density for time period (8 to 12 sec).

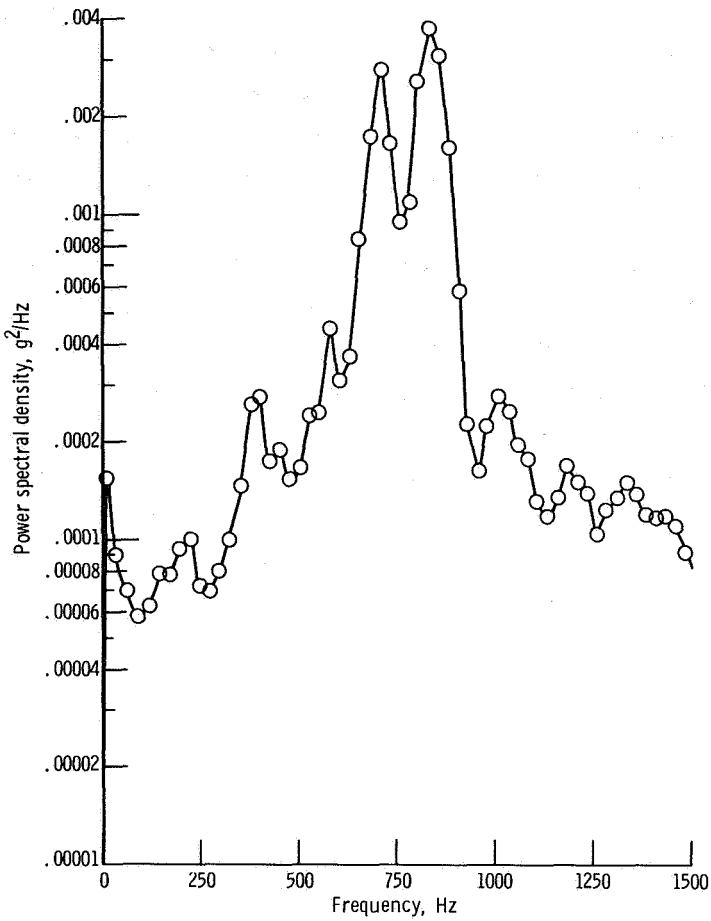

Figure 28. - Power spectral density for time period (12 to 20 sec).

The most significant data (fig. 25) from the vehicle viewpoint are obtained from accelerometer 6 mounted on the base ring of the payload experiment structure at station 177. This aluminum ring had a radial thickness of 2.5 inches (57.7 mm) and a longitudinal thickness of 1.6 inches (37 mm). The ring was clamped firmly to the upper flange of the spin isolator by the V-clamp (see fig. 6). However, it should be noted that the accelerometer measured the vibration input to the payload at the forward flange of the spin isolator and not at the second-stage motor thrust face.

Figure 26 shows that the highest g loads on the payload occurred at first-stage ignition, transonic flight (8 to 12 sec), second-stage ignition and near second-stage burnout (60 to 70 sec). Power spectral density and amplitude probability density analyses for accelerometer 6 were made during first-stage burn at two time periods (8 to 12 sec and 12 to 20 sec) and near second-stage burnout (63 to 68 sec) and are presented in figures 27 to 29.

The most severe g loads on the payload occurred during transonic flight. The total level as shown in figure 26 was 2.35 g's RMS with the energy being concentrated at 400, 700, and 825 hertz as seen in the power spectral density plot of figure 27. The energy at 400 hertz is due to first-stage motor excitation. The higher energy at 700 and 825 hertz is due to acoustic exci-

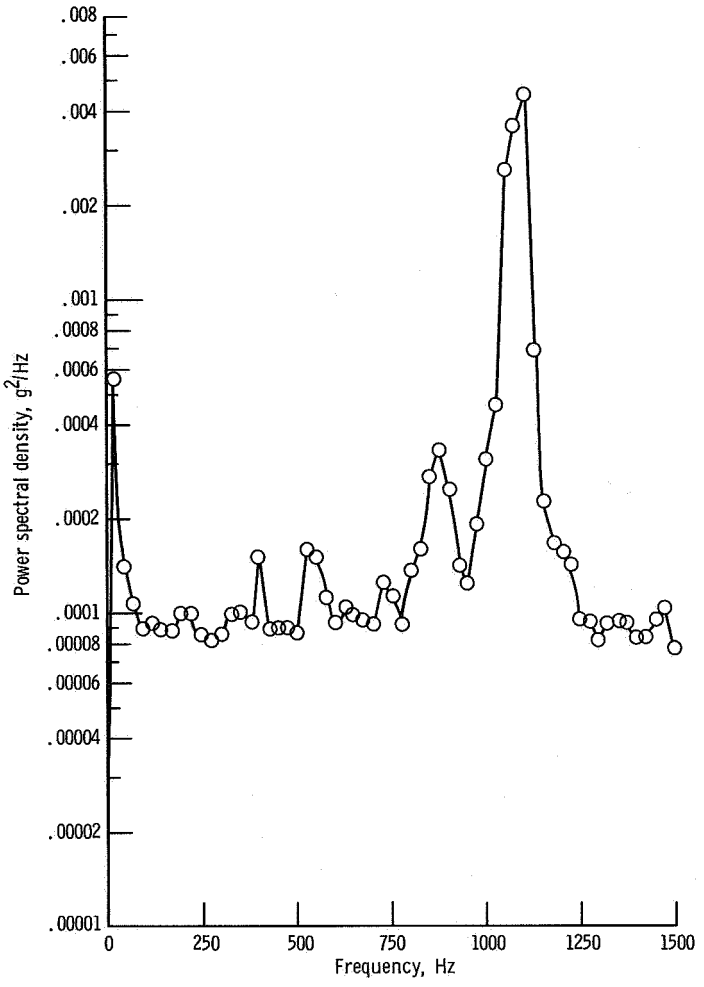

Figure 29. - Power spectral density for time period (63 to 68 sec).

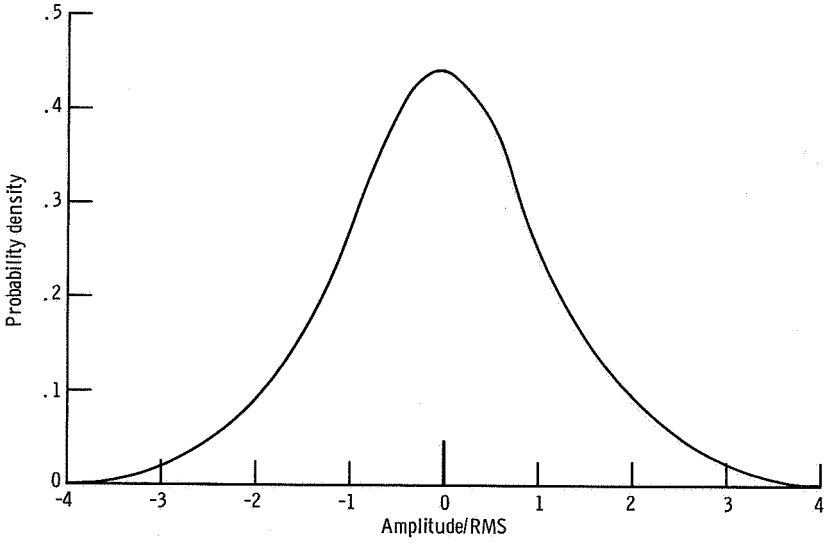

Figure 30. - Acceleration amplitude probability density time period (12 to 20 sec).

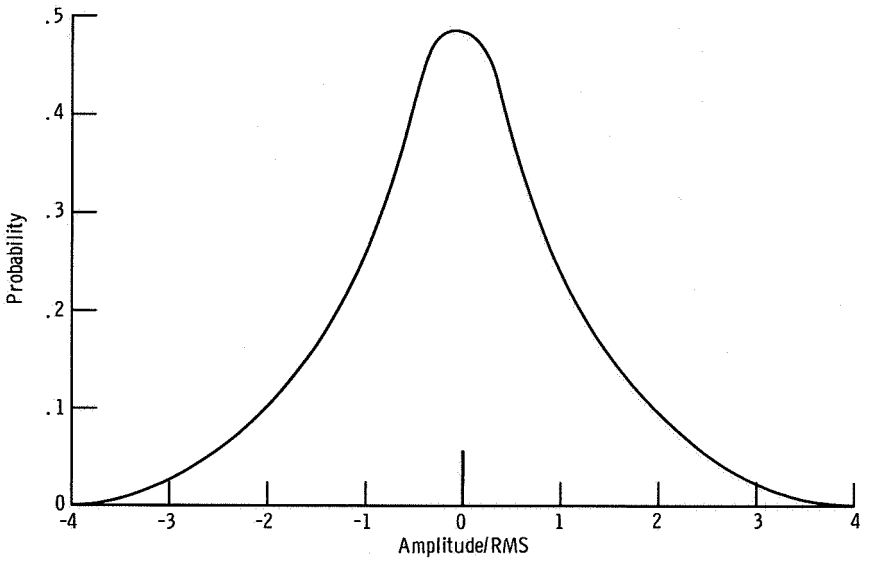

Figure 31. - Acceleration amplitude probability density time (8 to 12 sec).

tation. A comparison of figures 27 and 28 shows that, during the 8- to 12-second time period, the acoustic excitation was reduced by a factor of ten and the excitation at 400 hertz was reduced by one third, but that the frequency spectrum was generally the same. Figure 26 shows that the highest load during second-stage burn was 0.5 g RMS at 60 to 70 seconds with one predominant frequency at 1100 hertz as seen in figure 29. This energy is due to motor excitation.

The amplitude density plots (figs. 30 and 31) show the randomness of the data analyzed. The plots show no periodic components because of vehicle phenomenon or instrumentation error. The suspect inputs of engine and acoustic excitation should have a true Gaussian distribution which the APD plots approach.

CONCLUDING REMARKS

A general description of the design and construction of the WASP sounding rocket and of the performance of the first flight of the WASP sounding rocket are presented. The purpose of the flight test was to place the 862-pound (391-kg) spacecraft above 250 000 feet (76.25 km) on free-fall trajectory for at least 6 minutes in order to study the effect of "weightlessness" on a slosh dynamics experiment. The WASP sounding rocket fulfilled its intended mission requirements. The sounding rocket approximately followed a nominal trajectory. The payload was in free fall above 250 000 feet (76.25 km) for 6.5 minutes and reached an apogee altitude of 134 nautical miles (248 km).

Flight data including velocity, altitude, acceleration, roll rate, angle of attack, and flight vibrations are presented and discussed. The residual burning of the second-stage motor is presented and analyzed.

The longer than expected residual burning produced a calculated thrust level of 22.1 pounds (98.1 N) for a minimum of 23 seconds after nominal second-stage burnout. Analysis shows that the residual burning caused a minor collision between the separated spacecraft and the second stage.

Lewis Research Center,
National Aeronautics and Space Administration,
Cleveland, Ohio, September 13, 1967,
709-07-00-03-22.

REFERENCES

1. Gold, Harold; McArdle, Jack G.; and Petrash, Donald A.: Slosh Dynamics Study in Near Zero Gravity: Description of Vehicle and Spacecraft. NASA TN D-3985, 1967.
2. Pitts, William C.; Nielsen, Jack N.; and Kaattari, George E.: Lift and Center of Pressure of Wing-Body-Tail Combinations at Subsonic, Transonic, and Supersonic Speeds. NACA TR-1307, 1957.
3. Yuska, Joseph A.: Static Aerodynamic Characteristics of a Rocket Vehicle with Thick Wedge Fins and Sweptback Leading and Trailing Edges. NASA TN D-3182, 1966.
4. Falanga, Ralph A.; Hinson, William F.; and Crawford, David H.: Exploratory Tests of the Effects of Jet Plumes on the Flow Over Cone-Cylinder-Flare Bodies. NASA TN D-1000, 1962.
5. James, Robert L., Jr.; and Harris, Ronald J.: Calculation of Wind Compensation for Launching of Unguided Rockets. NASA TN D-645, 1961.
6. Anon.: U. S. Standard Atmosphere, 1962. NASA, USAF, and U. S. Weather Bureau, Dec. 1962.

NASA-Langley, 1968 — 31 E-4080